

# On Why and How Do Rivers Meander

14<sup>th</sup> IAHR Arthur Thomas Ippen Award Lecture, XXXI IAHR Congress, Seoul, South Korea, September 2005

A. M. FERREIRA DA SILVA, *Department of Civil Engineering, Queen's University, Kingston, Ontario, Canada. E-mail: amsilva@civil.queensu.ca*

*Mr. President,  
Dear colleagues,  
Ladies and gentlemen,*

*I am very honoured, and deeply grateful to the IAHR Awards Committee and the IAHR Council for making me the recipient of this year's Arthur Thomas Ippen Award.*

*It is a great pleasure for me to be here today to deliver this lecture. It has also been a great pleasure to attend this Congress, which was used as a special occasion to celebrate the 70<sup>th</sup> anniversary of IAHR – an association that is truly unique and exceptional in the many ways in which it supports us in our efforts to advance the state-of-the-art in research, teaching and practical application in all fields of hydraulics. Before turning to the topic of my lecture, I would like to wish IAHR, on its 70<sup>th</sup> anniversary, a long life! And may we continue to celebrate its anniversaries in the same spirit that animated us throughout this Congress.*

## **1. Introduction**

As is well known, meandering has attracted the attention of scientists and engineers since a long time. However, a systematic research on meandering appears to have been initiated towards the end of the 19<sup>th</sup> century (with, among others, the works of J. Thomson (see e.g. Ref. [45], from 1879), N. de Leliavsky (see e.g. Ref. [10], from 1894), M. Jefferson 1902, L. Fargue (see e.g. Ref. [14], from 1908), H. Engels 1926, etc.). Since then, a voluminous literature has been produced on various aspects of meandering streams (mechanics of meandering flows, initiation of meandering, time-growth of their loops, modelling of meandering streams, their bed topography, etc.), each of these aspects forming a separate and still ongoing research topic in its own right. [For reviews of past research on various meandering-related topics see e.g. Leliavsky 1959, Chang 1988 and Yalin 1992]. In my lecture today, I will focus on the present understanding of some aspects of meandering and especially give you our perspective. In particular, an attempt is made to answer the following questions: Why do rivers deviate from a straight alignment and start meandering? And how does a river evolve with the passage of time once meandering initiated?

In the first part of this lecture, and following da Silva (1991), Yalin (1992), the initiation of meandering and the subsequent time-growth of meander loops are explained in the light of recent discoveries in turbulence and the regime trend, respectively. In the second part, recent experimental findings regarding the convective behaviour of flow are used to explain characteristic features of the time-evolution of meander loops, including the variation with sinuosity of their speed of lateral expansion.

The above topics were extensively dealt with in the 2001 IAHR Monograph “Fluvial Processes” (Yalin and da Silva 2001). This lecture is used as an opportunity to further elaborate parts of the aforementioned monograph, as well as present additional information resulting from the author’s recent research.

## 2. Geometric Characteristics of Meandering Streams

Before proceeding further, the following pertinent aspects of the geometry of meandering streams – invoked throughout this lecture – should be mentioned.

### 2.1 Meander wavelength

**i)** Several authors, and most prominently Inglis (1947), Leopold and Wolman (1957), and Zeller (1967), realized long ago that the meander wavelength  $\Lambda_M$  (see the definition sketch in Fig. 1) is related to the flow width  $B$  by a simple proportionality, i.e. that  $\Lambda_M = nB$ . Fig. 2, which is the extended version of Fig. 13.12 in Ref. [17], shows the plot of the meander wavelength data from various sources versus flow width. This Figure indicates that  $n \approx 6$ , and thus that the (average) meander wavelength  $\Lambda_M$  can best be given by

$$\Lambda_M \approx 6B. \quad (1)$$

**ii)** Observe that Fig. 2 contains data not only from alluvial streams, but also from meltwater channels on ice and meanders on the Gulf Stream. These data are from Leopold *et al.* (1964), who appear to have been the first to realize that “the meander pattern of meltwater channels on the surface of glaciers have nearly identical geometry to the meander bends in rivers” and that “the geometry in plan view of meanders in the Gulf Stream is also similar to that of rivers”. It should be noted that, as pointed out by Leopold *et al.* (1964), p. 302, the “meandering channels on ice are formed without any sediment load or point-bar construction by sediment deposition” and that the meanders on the Gulf Stream too occur “... without debris load and, in this instance, without confining banks”. Considering this, Yalin (1992), p. 161, defined meandering as a “*self-induced* plan deformation of a stream that is (ideally) periodic and anti-symmetrical with respect to an axis,  $x$  say, which may or may not be exactly straight”. The term self-induced is used to imply that the deformation is induced by the stream itself, as opposed to being “forced” upon the stream by its environment.

**iii)** From a very large number of field and laboratory measurements carried out mostly by Japanese researchers (see e.g. Hayashi 1971, JSCE 1973), it follows that the average length  $\Lambda_a$  of alternate bars (see Fig. 6(b) later on, showing a plan view of alternate bars and definition of  $\Lambda_a$ ) is approximately equal to six times the flow width. Note the striking similarity between  $\Lambda_M$  and  $\Lambda_a$ :

$$\Lambda_M \equiv \Lambda_a \approx 6B. \quad (2)$$

### 2.2 Plan shape of a meandering stream; Sine-generated curve

It appears to be generally accepted nowadays that the centreline (in plan view) of a natural regular meandering stream is best idealized by the sine-generated curve (due to Leopold and Langbein 1966, Langbein and Leopold 1966). As is well known, this periodic (along the general flow direction  $x$ ) curve is determined by the following equation

$$\theta = \theta_0 \cos\left(2\pi \frac{l_c}{L}\right), \quad (3)$$

(see List of Symbols and Fig. 1 for the meaning of symbols in this equation).

From Eq. (3) it should be clear that a fundamental property of sine-generated channels is that they exhibit a continuous variation of the centreline curvature  $1/R$  ( $= -d\theta/dl_c$ ) along the streamwise direction  $l_c$ : at crossovers  $O_i$ , where  $l_c = 0, L/2, L, \dots$ , etc., then  $|1/R| = 0$ ; at apexes  $a_i$ , where  $l_c = L/4, 3L/4, 5L/4, \dots$  etc., then  $|1/R|$  is maximum.

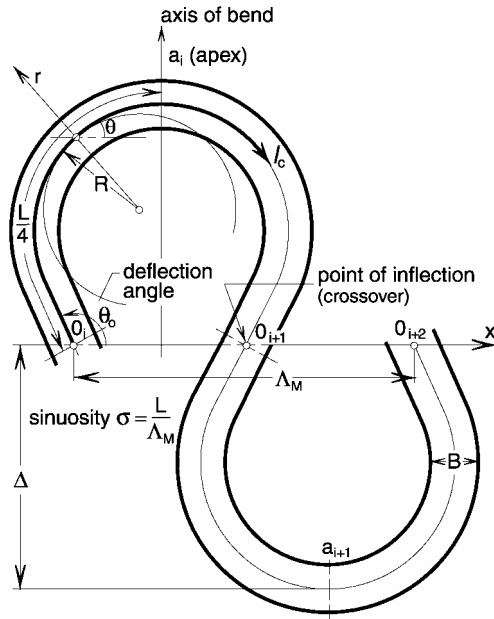


Figure 1 Definition sketch

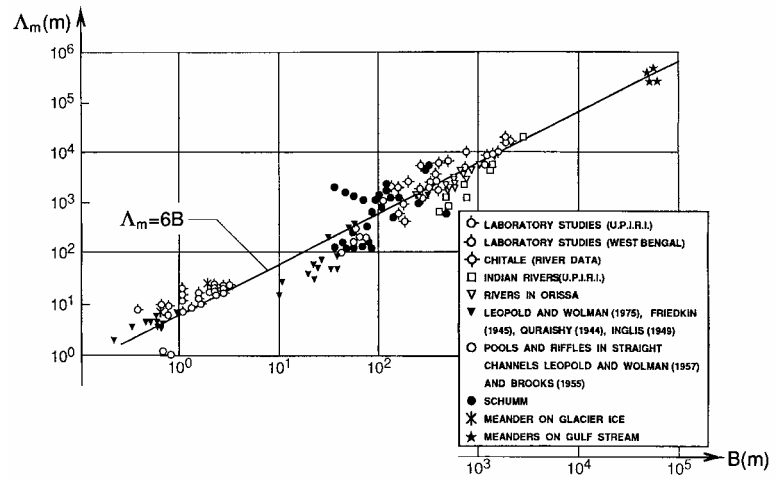


Figure 2 Plot of meander wavelength versus flow width (after Garde and Raju 1977)

The sinuosity  $\sigma = L/\Lambda_M$  and the dimensionless curvature at the apex  $B/R_a$  of sine-generated channels are uniquely determined by  $\theta_0$  as  $\sigma = 1/J_0(\theta_0)$  and  $B/R_a = \theta_0 J_0(\theta_0)$ , where  $J_0(\theta_0)$  is the Bessel function of first order and zero-th kind of  $\theta_0$  (Yalin 1992). The first of these relations implies that the different sine-generated plan shapes are due to the different values of the deflection angle  $\theta_0$  only. The graphs of  $1/\sigma$  and  $B/R_a$  are shown in Fig. 3(a). Observe that the largest values of (dimensionless) curvature at the apex occur for intermediate values of  $\theta_0$  ( $\theta_0 \approx 70^\circ$ ), and that  $B/R_a$  then gradually decreases with the increment of deviation of  $\theta_0$  from  $\approx 70^\circ$ . The maximum possible value of  $\theta_0$  is  $\approx 138^\circ = 2.41 \text{ rad}$ . This corresponds to  $J_0(\theta_0) = 0$  and  $L, \sigma \rightarrow \infty$ . However, in practice, this can never occur, for when  $\theta_0$  reaches the value  $\approx 126^\circ = 2.20 \text{ rad}$  ( $\sigma \approx 8.5$ ), the meander loops come into contact with each other and the meandering pattern is destroyed (Fig. 3(b)).

### 3. Large-scale Turbulence and the Initiation of Meandering

The reason for why rivers meander has been a subject of intensive debate in the literature, with many ideas and suggestions emerging over the past 100 years (Coriolis force, bank erosion due to local disturbances, theory of most probable path, unstable response of the banks to a small-amplitude perturbation, alternate bars, etc.). According to Yang (1971), most theories “emphasize some special

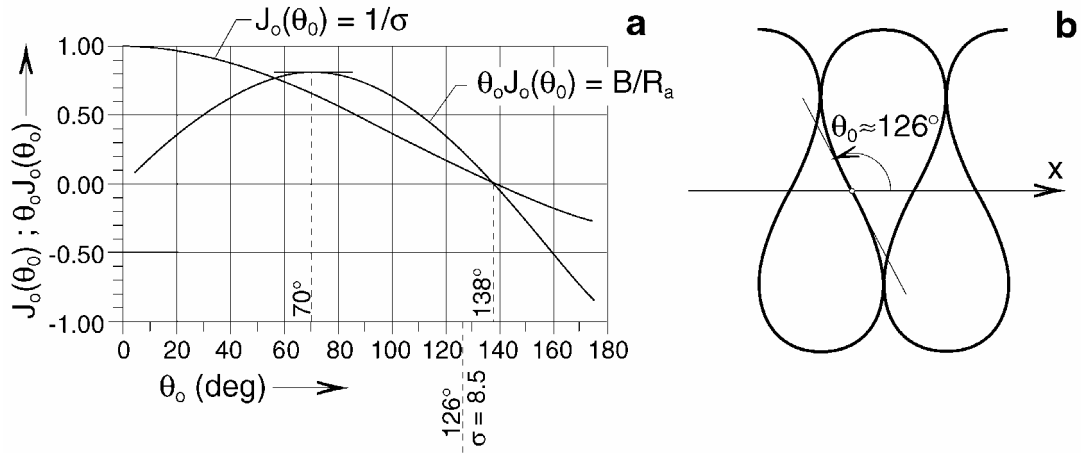


Figure 3 Geometric characteristics of sine-generated meandering streams. (a) Plot of  $1/\sigma$  and  $B/R_a$  versus  $\theta_0$ ; (b) Maximum possible value of  $\theta_0$

phenomena observed in meandering channels and neglect the physical reasoning which creates them". From the debates of these theories, eventually the idea settled that if an explanation for why meandering initiates is to be generally accepted, it should not fail to explain: 1- why the wavelength of meanders should be  $\Lambda_M \approx 6B$ , and 2- why meanders occur even when there is no sediment transport (see Section 2). The view that meandering is caused by the large-scale turbulence, expressed by many prominent researchers dealing with fluvial processes (Leopold 1957, Velikanov 1958, Karcz 1971, Yalin 1977, Grishnanin 1979, etc.), appears to stem from the realization of these two facts. However, this view could not be satisfactorily demonstrated until the relatively recent discovery of bursting processes. In this Section, bursting processes are described in a schematical manner – all possible deviations and distortions due to the strong “random element” ever-present in any turbulent flow are disregarded in this description. An outline of the initiation of meandering by bursts is given in Section 4.

### 3.1 Coherent structures and bursts

Following Hussain (1983), the term “coherent structure” (CS) is used here to designate the largest conglomeration of turbulent eddies which has a prevailing sense of rotation, the term burst, to designate the evolution of a CS during its life-span  $T$ . The bursts can be vertical ( $V$ ) or horizontal ( $H$ ). The CS's of the former rotate in the  $(x; z)$ -planes, those of the latter, in the  $(x; y)$ -planes (Fig. 4).

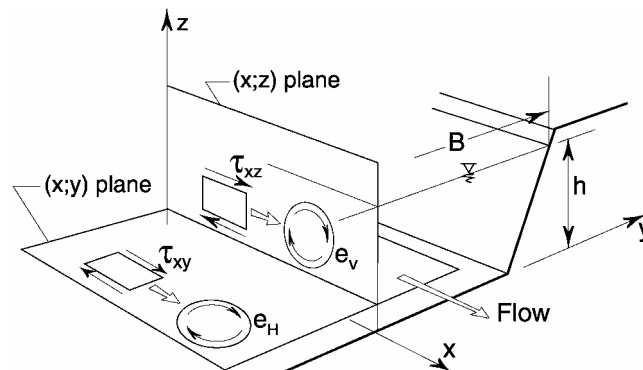


Figure 4 Vertical and horizontal planes of rotation of CS's

It is not yet known how exactly the aforementioned CS's originate and develop and the following is a brief "synthesis" of the contents of Blackwelder (1978), Grishanin (1979), Cantwell (1981), Hussain (1983), Gad-el-Hak and Hussain (1986), Rashidi and Banerjee (1988), and several others.

i) A vertical burst-forming CS originates at a location around a point  $P$  (at  $O_i$ ; see Fig. 5(a)) near the flow boundary. At  $t = 0$ , a future macroturbulent eddy  $e_V$  ("transverse vortex") rolls-up at  $P$  (which is assumed to be at  $x = 0$ ), and it is ejected, together with the fluid under it, away from the bed. This total fluid mass moves towards the free surface, as it is conveyed by the flow downstream (*ejection phase*). In the process, the moving fluid mass continually enlarges (by engulfment) and new eddies  $e'_V, e''_V, \dots$ , are generated (by induction) – thus a continually growing CS comes into being. When this structure becomes as large as to touch the free surface, it disintegrates (*break-up phase*) into a multitude of smaller and then even smaller eddies ... until their size becomes as small as the lower limit  $\nu/\nu_*$ , where their energy is dissipated (as implied by the "Eddy-Cascade Theory"). The neutralized fluid mass moves then downstream – towards the bed (*sweep stage*), with a substantially smaller velocity than that of ejection. At  $t = T_V$ , the fluid arrives at  $x = \lambda_V$ , which prompts the initiation of the "new" cycle at the next downstream point  $P$  (Hussain 1983, Nezu and Nakagawa 1993, etc.). The above described cycle is referred to as *burst-cycle*, or simply, as *burst*.

The conceptual Fig. 5(a) shows (in a stationary frame) a  $V$ -burst cycle of an open-channel flow; the cine-record in Fig. 5(b) shows (in a convective frame) an instantaneous view of two consecutive CS's.

ii) The analogous is valid, *mutatis mutandi*, for an  $H$ -burst. The difference appears to be in the length scale: all "lengths" of the large-scale vertical turbulence are proportional to the flow depth  $h$ ; those of the large-scale horizontal turbulence, to the flow width  $B$ . The burst-forming HCS's extend (along  $z$ )

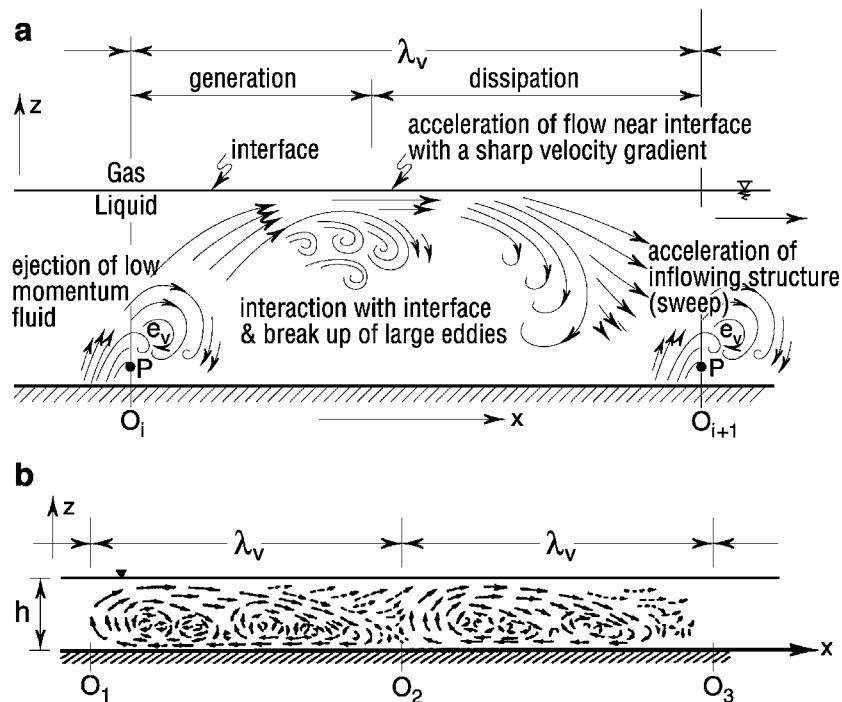


Figure 5 (a) Conceptual representation of a  $V$ -burst cycle (after Rashidi and Banerjee 1988); (b) Cine-record showing an instantaneous view of two consecutive CS's (from Klaven 1966)

throughout the flow thickness  $h$ , and they can thus be likened to thin horizontal “disks” (Yokosi 1967).

The HCS's originate at the points  $O_i$  near the banks (see Fig. 6(a)) and the free surface, where horizontal shear stresses  $\tau_{xy}$  are the largest. Afterwards, they are conveyed by the mean flow downstream, while growing in size. Provided that the width-to-depth ratio is not too “large” (see Section 4, paragraph (iii)), then the HCS's will grow until their lateral extent becomes as large as  $B$ . At this point, they interact with the opposite bank and disintegrate. The neutralized fluid mass returns to its original bank so as to arrive there at  $t = T_H$ . It is likely that if the bursts are “fired” from the points  $O_1, O_2, \dots$  at the times  $t = 0, 1, 2, \dots$ , say, then at the points  $O'_1, O'_2, \dots$  they are “fired” at  $t = 1/2, 3/2, \dots$  (see da Silva 1991).

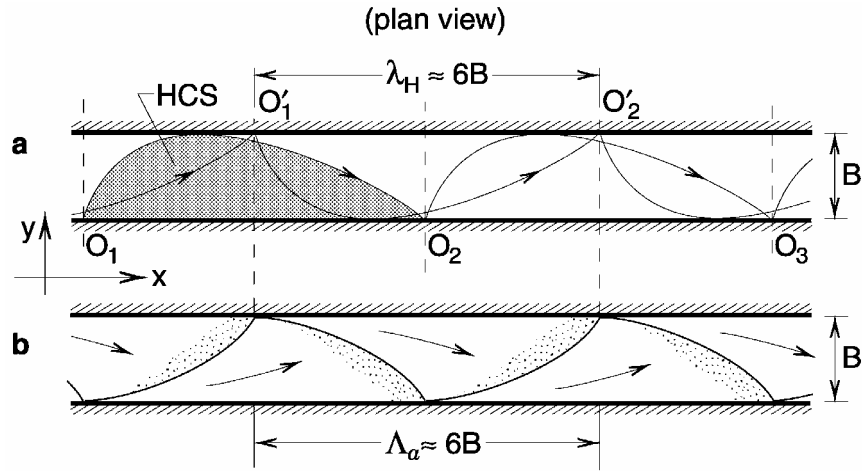


Figure 6 (a) Plan view of sequences of HCS's; (b) Plan view of alternate bars

iii) If  $O_i$  and  $O_{i+1}$  are the “birth-places” of two consecutive bursts of a burst-sequence (Figs. 5(a) and 6(a)), then the distance  $O_i O_{i+1} = \lambda_V$  or  $\lambda_H$  is the burst-length, the life-span of a burst being  $T_V = \lambda_V / u_{av}$  or  $T_H = \lambda_H / u_{av}$  (for CS's are transported by the flow with the velocity  $\approx u_{av}$ ). Let  $O_0$  be the origin of the first burst of a burst-sequence. If  $O_0$  is fixed (e.g. if  $O_0$  is the location of the “local discontinuity”  $\delta$  in the sense of Yalin 1992), then the rest of  $O_i$ 's must also be considered as fixed, for each of them is distant from  $O_0$  by an integer number of the constant lengths  $\lambda_V$  and  $\lambda_H$ . But this means that the straight time-average initial flow is subjected to a perpetual action of bursts “fired” from the (ideally speaking) same location  $O_i$ . This action must inevitably render the flow to acquire a sequence of periodic (along  $x$  and  $t$ ) non-uniformities, which, in turn, must cause, by virtue of the sediment transport continuity equation, the emergence of the periodic (along  $x$ ) bed- and/or bank-forms ( $j$ ). These initial forms must grow with the passage of time (by coalescence) until they acquire their developed length  $\Lambda_j$  that is the same as the burst length:

$$\Lambda_j = \lambda_V \text{ or } \lambda_H. \quad (4)$$

iv) The burst lengths  $\lambda_V$  and  $\lambda_H$  are found to be independent of the inner variables  $v_* k_s / \nu$  and  $k_s / h$ : they scale, respectively, with the outer variables  $h$  and  $B$  (see e.g. Nezu and Nakagawa 1993, Gad-el-Hak and Hussain 1986, Cantwell 1981). Indeed, as can be noted e.g. from Figs. 2.4(a) and (b)

in Yalin and da Silva (2001), the data-points of  $\lambda_V / h$  cluster at the level  $\approx 6$ , irrespective of what the value of  $Re = u_{av} h / \nu$  ( $= c(h/k_s)(v_* k_s / \nu)$ ) might be. Thus

$$\frac{\lambda_V}{h} \approx 6. \quad (5)$$

Similarly, the oscillograms recorded by Yokosi (1967) in Uji River, Japan, and those obtained by Dementiev (1962) in Syr-Darya River, former U.S.S.R. (and reproduced in Figs. 3.15 and 3.16 in da Silva 1991 and Figs. 2.18 to 2.20 in Yalin 1992) indicate that the dimensionless  $\lambda_H$ , viz  $\lambda_H / B$ , can also be expressed as

$$\frac{\lambda_H}{B} \approx 6. \quad (6)$$

However, as will be presently clarified, the relation (6) is valid only if the aspect ratio ( $B/h$ ) of the flow does not exceed a certain upper limit.

#### 4. On the Initiation of Meandering by the Large-Scale Horizontal Turbulence

In the following, we will focus exclusively on horizontal bursts and their consequences. (Those interested in the effect of vertical bursts on the movable bed, namely the emergence of bed forms of the length  $\Lambda_d \approx 6h$  (that is, dunes), are referred to Yalin 1992).

i) From the content of the previous section, it follows that

$$\lambda_H \equiv \Lambda_a \equiv \Lambda_M \approx 6B. \quad (7)$$

The remarkable coincidence between the (average) horizontal burst length  $\lambda_H$ , the (average) alternate bar length  $\Lambda_a$ , and the (average) meander wavelength  $\Lambda_M$  implied by (7) suggests that both alternate bars and meanders initiate because of the same mechanism, namely horizontal bursts. Alternate bars are due to the action of horizontal bursts on the deformable surface of the movable bed, the initiation of meandering being due to the action of horizontal bursts on the deformable banks. In the following, the conditions under which horizontal bursts may lead to meandering and/or to alternate bars are discussed.

ii) Consider a straight and prismatic open-channel, having a rectangular cross-section ( $B_0 \times h_0$ ). The granular bed is flat and its roughness is  $k_s$ . The steady and uniform flow, which commences at  $t = 0$ , is rough turbulent. The turbulence structure of this flow can be affected only by the channel geometry and its roughness. i.e. this structure is completely determined by the parameters  $B$ ,  $h$  and  $k_s$  ( $\sim D$ ) and thus by the dimensionless variables  $B/h$  and  $h/k_s$  (or, equivalently,  $h/D$ ). Hence it would be only appropriate to locate the existence regions of various types of alluvial forms (bed and plan forms) due to horizontal macroturbulence, and in particular alternate bars and meanders, on the ( $B/h; h/D$ )-plan. Accordingly, the  $B/h$ - and  $h/D$ -values of all the available field and laboratory data are plotted in Fig. 7 (The References to the data in this Figure are given in Yalin and da Silva 2001, at the end of Chapter 4). Observe from this graph that the upper boundary of the existence

region of alternate bars, namely the line  $\mathcal{L}$ , can be taken (approximately) as the upper boundary of the existence region of meanders. However, the lower boundaries of the existence regions of alternate bars and meanders are different. The lower boundary of the alternate bar region is the line  $\mathcal{L}_A$ ; the lower boundary of the meandering region is the line  $\mathcal{L}_M$ .

iii) From the aforementioned it follows that:

1. If  $B/h$  is small (smaller than the ordinates of the line  $\mathcal{L}_A$ ), then the horizontal burst-forming coherent structures grow until their lateral extent becomes as large as  $B$  without rubbing the bed (like in Fig. 8(b)), and therefore they cannot produce “their” bed forms, viz alternate bars. Yet, the sequence of these structures can still initiate meandering by their direct impact on the banks, and/or by the convective action of the internal meandering they generate. Thus the horizontal bursts can “imprint” on the channels banks the length  $\lambda_H \approx 6B_0$ , without alternate bars. This occurs in the zone between the lines  $\mathcal{L}_A$  and  $\mathcal{L}_M$ . Fig. 9(a) shows how the sequence of horizontal bursts of an initial channel causes the flow and the alluvial banks to deform (in plan view) in a wave-like manner.

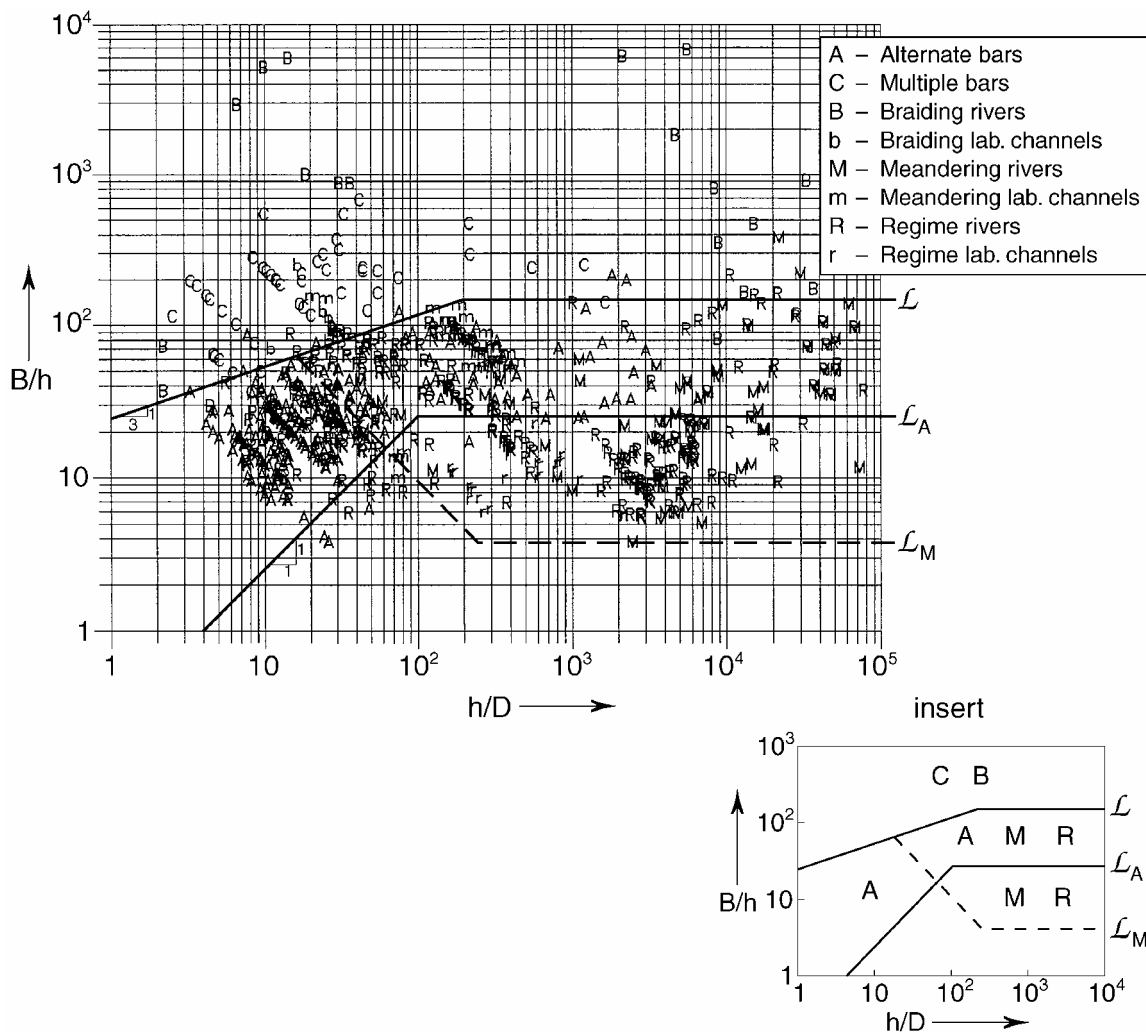


Figure 7 ( $B/h; h/D$ )-plan defining the existence regions of alluvial forms due to horizontal macroturbulence

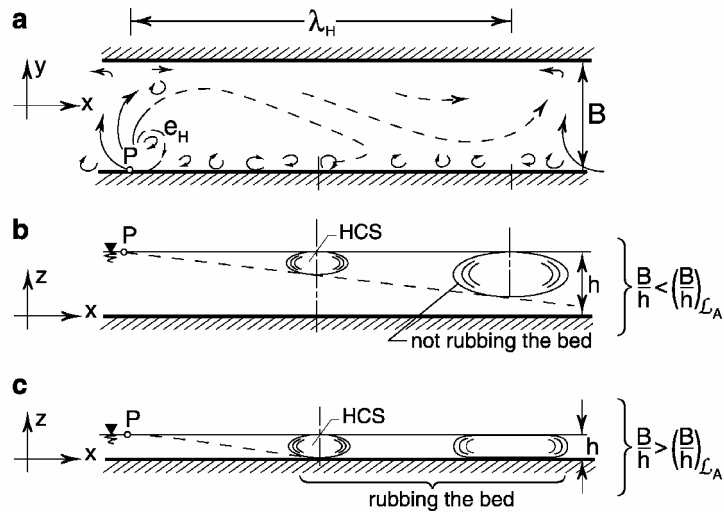


Figure 8 Evolution of a HCS. (a) Plan view; (b) and (c) Longitudinal views, corresponding to the cases where the HCS is not rubbing the bed and is rubbing the bed, respectively

- If  $B/h$  is larger than the ordinates of  $\mathcal{L}_A$ , but smaller than those of  $\mathcal{L}$ , then the horizontal coherent structures are rubbing the bed (like in Fig. 8(c)), and they produce first the alternate bars (as shown in Fig. 6). These act as “guide-vanes”, facilitating (accelerating) the bank deformation which would have occurred anyway due to direct impact of HCS’s on the banks. In this case, the points A and M can be present in the same zone (viz between the lines  $\mathcal{L}$  and  $\mathcal{L}_A$ ).

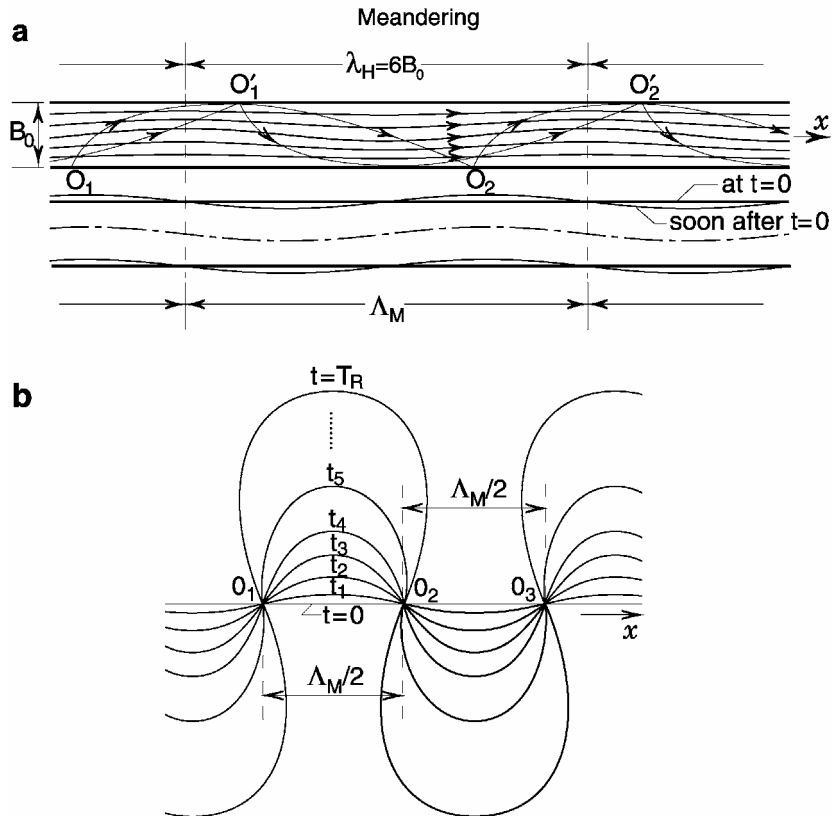


Figure 9 Initiation and subsequent development of meanders

[If  $B/h$  is larger than the ordinates of  $\mathcal{L}$ , then the horizontal bursts emitted from one bank will not be able to grow as to reach the opposite bank, for they will be destroyed before that by friction. In this case, the horizontal coherent structures issued from both banks may meet each other in the midst of the stream, or even not be able to meet at all. Thus instead of the one-row burst configuration and one-row bars (alternate bars) like in Fig. 6, we will have 2-row burst configuration and 2-row bars, or 3-row burst configuration and 3-row bars, etc. The formation of n-row bars (multiple bars) by n-row burst configurations and its relation to braiding is discussed elsewhere (Yalin 1992, Yalin and da Silva 2001).]

## 5. Regime Development and Time-Growth of Meander Loops

i) Regime (or stable) channels and meandering have usually been regarded and treated as independent fluvial phenomena. We owe the first suggestions that the phenomena mentioned may not really be independent to Bettess and White (1983) and Chang (1988). An outline of the time-growth of meander loops in the light of the regime-trend following da Silva (1991), Yalin (1992) and Yalin and da Silva (2001) is given below.

ii) Consider an experiment which starts at  $t=0$  in a straight initial channel excavated in an alluvial valley. The slope  $S_0$  of the initial channel is the same as the valley slope  $S_v$ , i.e.  $S_0 = S_v$ . It is assumed that the granular material and fluid are specified, that the flow rate  $Q$  is given ( $Q = Q_{bf} = const$ ,  $Q_{bf}$  being the bankfull flow rate), and that the conditions are such that sediment can be transported. It is also assumed that the initial channel  $(B_0, h_0, S_0)$  is such that the formation of the regime channel  $(B_R, h_R, S_R)$  is possible. The duration of formation of the regime channel is  $T_R$ .

The laboratory research (see e.g. Ackers 1964, Leopold and Wolman 1957) indicates that the variation of the flow width  $B$ , the flow depth  $h$ , and the slope  $S$  during  $T_R$  takes place as shown in the schematic Fig. 10. In the (very short) part  $\hat{T}_0$  of  $T_R$ ,  $B$  and  $h$  vary substantially, while  $S$  remains nearly constant ( $S \approx S_0$ ); no regime development as such takes place. The part  $\hat{T}_0$  of  $T_R$  is merely the duration needed to alter (the arbitrary)  $B_0$  and  $h_0$  into such  $\hat{B}_0 (\approx B_R)$  and  $\hat{h}_0$ , say, which are in equilibrium with the existing  $S \approx S_0$  and which together with  $S_0$  are able to convey the given flow rate  $Q$ . The regime development in the proper sense takes place only after the *adjustment period*  $\hat{T}_0$ . (The time  $t=0$  in the previous section is to be identified with the present  $t = \hat{T}_0$ ).

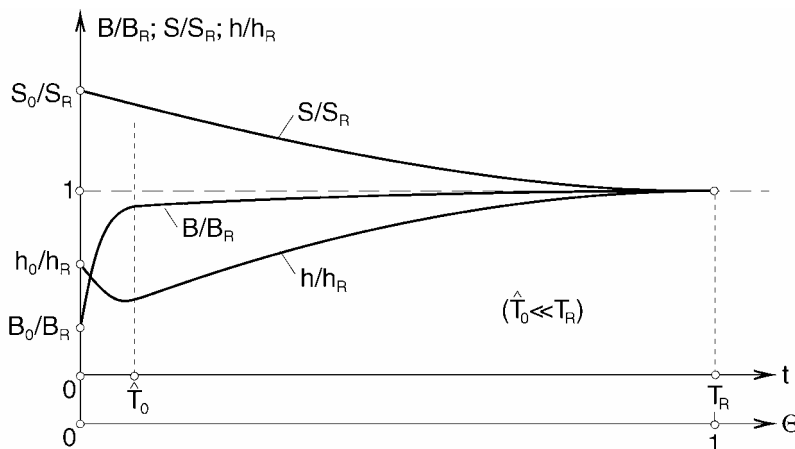


Figure 10 Schematic representation of regime development with time of flow width  $B$ , flow depth  $h$ , and slope  $S$

According to the contemporary rational approaches to regime, the regime development is a process in which the stream appropriately alters its channel so that a certain energy-related quantity,  $A_*$  say, may be minimized. Although different authors proposed different quantities as  $A_*$  (e.g. according to Chang 1988,  $A_* = \gamma QS$ ; according to Yang *et al.* 1981,  $A_* = u_{av} S$ ; according to Jia 1990 and Yalin 1992,  $A_* = Fr$ , where  $Fr \sim S$ ; according to Yalin and da Silva 2001,  $A_* = u_{av}$ ), almost invariably  $A_*$  is such that its minimization can only be achieved through the decrement of the slope. This is in agreement with the aforementioned experimental observations.

Clearly, the decrement of the slope (from  $S_0$  to  $S_R$ ) can only be achieved either by degradation-aggradation, or by meandering (for the expansion of meander loops (see Fig. 9(b)), i.e. the increment of their length, means the decrement of the channel slope) – or by a combination of both. The development stops, and thus the expansion of meander loops stops, at  $t = T_R$  when  $S = S_R$ . In the case of large sand-bed rivers, the regime development is accomplished primarily by meandering. For the regime slope of large sand-bed rivers is usually rather small and, as pointed out by Chang (1988), “reduction of channel slope through incision would require tremendous degradation. For these reasons, the river channel usually adjusts by developing a flatter slope through meandering” (p. 313).

## 6. Convective Flow and Deformation of Bed and Banks

As is well known, at the same time that meander loops expand, they also migrate downstream. (Since loops expand by maintaining the distance between consecutive crossovers  $O_1, O_2, O_3, \dots$  (see Fig. 9(b)), downstream migration was disregarded in the previous section so as not to encumber the explanations). The evolution in plan of meander loops through (simultaneous) downstream migration and loop expansion is illustrated in Fig. 11, where the results of one of the laboratory runs by Friedkin (1945) are shown.

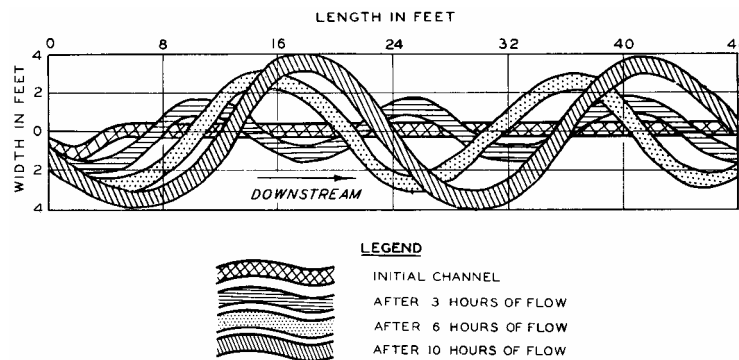


Figure 11 Evolution of a meandering stream through downstream migration and lateral expansion (from Friedkin 1945)

From field measurements in European and American rivers, but especially from series of river surveys carried out over long periods of time in Russian rivers including the Dnieper, Oka, Irtish, etc. (compiled and analysed by Kondratiev *et al.* 1982), it follows that the (normalized) migration velocity and the expansion speed of freely meandering rivers varies with  $\theta_0$  as shown schematically in Fig. 12. “At the early stages (small  $\theta_0$ ), it is the downstream migration of the meander waves which is mainly observable, at the latter stages (large  $\theta_0$ ), it is their expansion which dominates” (Kondratiev *et al.*, p. 108).

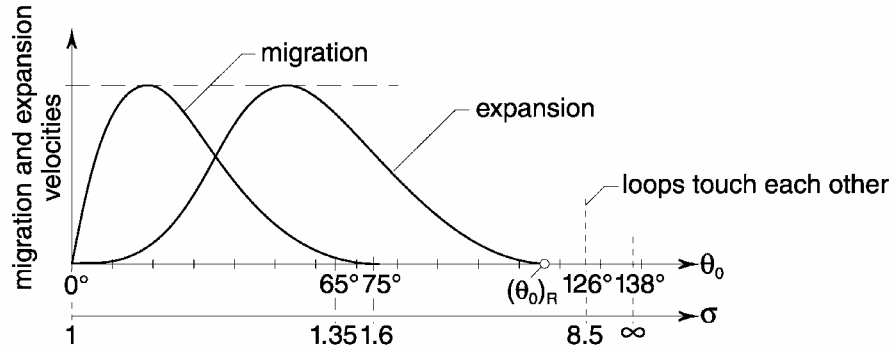


Figure 12 Schematic plot of (normalized) migration and expansion velocity of meander loops versus  $\theta_0$

In the following, the patterns of migration and expansion described above are explained on the basis of the convective behaviour of the flow. It will be assumed that the plan shape of the stream is sine-generated, that its width-to-depth ratio  $B/h$  is “large” ( $>\approx 20$ , say), and that the flow is turbulent and sub-critical. The assumption that  $B/h$  is “large” gives the possibility to replace the consideration of an actual 3D-stream by that of its *vertically-averaged* 2D counterpart (as has been successfully done already by several authors (see Kalkwijk and De Vriend 1980, Smith and McLean 1984, Nelson and Smith 1989, Struiksmas and Crosato 1989, Shimizu 1991, etc.)). This assumption also conveys that the role of the cross-circulation ( $\Gamma$ ) is negligible with regard to the present considerations. Indeed the relation

$$\left(\frac{\bar{v}'_{\Gamma}}{\bar{u}}\right)^2 = \alpha c_{av}^2 [\theta_0 J_0(\theta_0)] \sin\left(2\pi \frac{l_c}{L}\right) \cdot \frac{h_{av}}{B} \quad (8)$$

(derived in Yalin & da Silva 2001, pp. 136 to 140) indicates that  $\bar{v}'_{\Gamma}/\bar{u} \rightarrow 0$  when  $B/h_{av} \rightarrow \infty$ , and thus that  $\Gamma$  ( $\sim \bar{v}'_{\Gamma}$ ) can be ignored when  $B/h_{av}$  is “large”. The irrelevance of  $\Gamma$  with regard to the formation of wide natural streams has been independently pointed out in the past by many eminent field-research engineers (such as Leliavsky 1959, Matthes 1941, Kondratiev *et al.* 1982, Velikanov 1955 and Makaveyev 1975). [More on the topic in Chapter 5 of Yalin & da Silva 2001; see also Hooke 1974].

**i)** Consider the flow in a wide meandering (sine-generated) channel at the beginning of experiment (at the time  $t = 0$ ): the channel bed is *flat* (it is the graded surface of a mobile bed). From experiment and numerical simulations, it is known that the vertically-averaged streamlines  $s$  of this (*initial*) flow are not parallel: in some parts of the flow-plan they converge, in some others they diverge from each other (Fig. 13). At any given flow cross-section, if the  $Q/2$ -flow on one side of  $s_*$  is accelerating (and the vertically-averaged streamlines  $s$  are converging to each other), then the  $Q/2$ -flow on the other side of  $s_*$  is decelerating (and the vertically-averaged streamlines  $s$  are diverging from each other). As a consequence the streamlines  $s$  form, in the flow plan, adjacent to each other convergence and divergence flow zones as shown schematically in Fig. 13. In the case of a sine-generated stream, the convergence-divergence zones have the length  $L/2$  and periodically alternate along  $l_c$ .

In the following, the deviation angle between the vertically-averaged streamlines and the longitudinal coordinate lines will be termed  $\bar{\omega}$ .

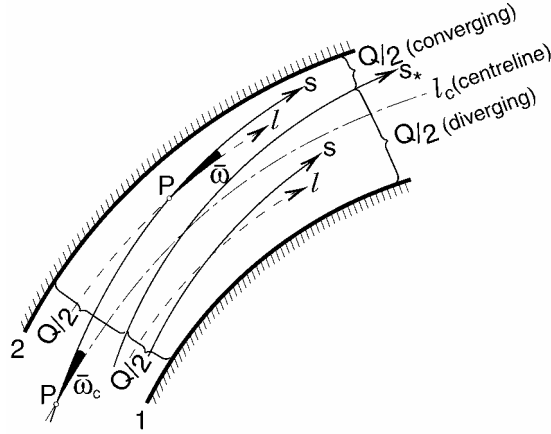


Figure 13 Convergence-divergence zones of meandering flows

ii) Since the local sediment transport rate  $q_s$  is an increasing function of the (local) vertically-averaged flow velocity  $\bar{U}$ , the convective variation of  $\bar{U}$  in a flow zone must inevitably cause the corresponding convective variation of  $q_s$  in that zone; i.e. it must cause the scalar  $\nabla \mathbf{q}_s$  to acquire a non-zero value. But  $\nabla \mathbf{q}_s \neq 0$  must, in turn, induce the displacement of the bed surface in vertical direction ( $z$ ) – as required by the sediment transport continuity equation

$$W = (1 - p) \frac{\partial z_b}{\partial t} = -\nabla \mathbf{q}_s, \quad (9)$$

where  $W$  is the vertical displacement velocity of the bed surface. This equation indicates that if  $\nabla \mathbf{q}_s > 0$ , then  $W < 0$  (erosion), and if  $\nabla \mathbf{q}_s < 0$ , then  $W > 0$  (deposition). Only in the locations where the flow is parallel, and thus  $\nabla \mathbf{q}_s = 0$ , the elevation  $z_b$  of the bed surface can remain unchanged ( $W = 0$ ).

It follows that the zones of the downward and upward bed displacements (i.e. the erosion and deposition zones) must necessarily coincide with the zones of convective acceleration and deceleration of flow, respectively.

iii) The deformed bed of a meandering stream consists of a longitudinal sequence of laterally adjacent “deeps” and “hills”. Each (deep) + (hill) complex can be viewed as one erosion-deposition zone (in short [ED]). From the preceding section it should be clear that each [ED] is brought into being by a (corresponding) convergence-divergence zone (in short, by [CD]) of the initial flow. Hence the length of each [ED] must be the same as that of each [CD], viz  $L/2$ .

From laboratory measurements of sine-generated meandering flows having a flat bed and “small” and “large” values of  $\theta_0$  (see Whiting and Dietrich 1993, da Silva 1995, Termini 1996), it follows that:

1. If  $\theta_0$  is “small” (Fig. 14(a)), then a [CD] exhibiting (throughout its length)  $\bar{\omega} > 0$ , extends between the apex-sections  $a_i$  and  $a_{i+1}$  (where the value of  $\bar{\omega}$  is zero), the most intense convergence/divergence ( $\bar{\omega}_{\max}$ ) being at the crossover-section  $O_{i+1}$ ;
2. If  $\theta_0$  is “large” (Fig. 14(b)), then the analogous [CD] exhibiting  $\bar{\omega} > 0$  extends approximately between the crossover-sections  $O_i$  and  $O_{i+1}$  (where  $\bar{\omega} = 0$ ), the most intense convergence/divergence ( $\bar{\omega}_{\max}$ ) being at the apex-section  $a_i$ .

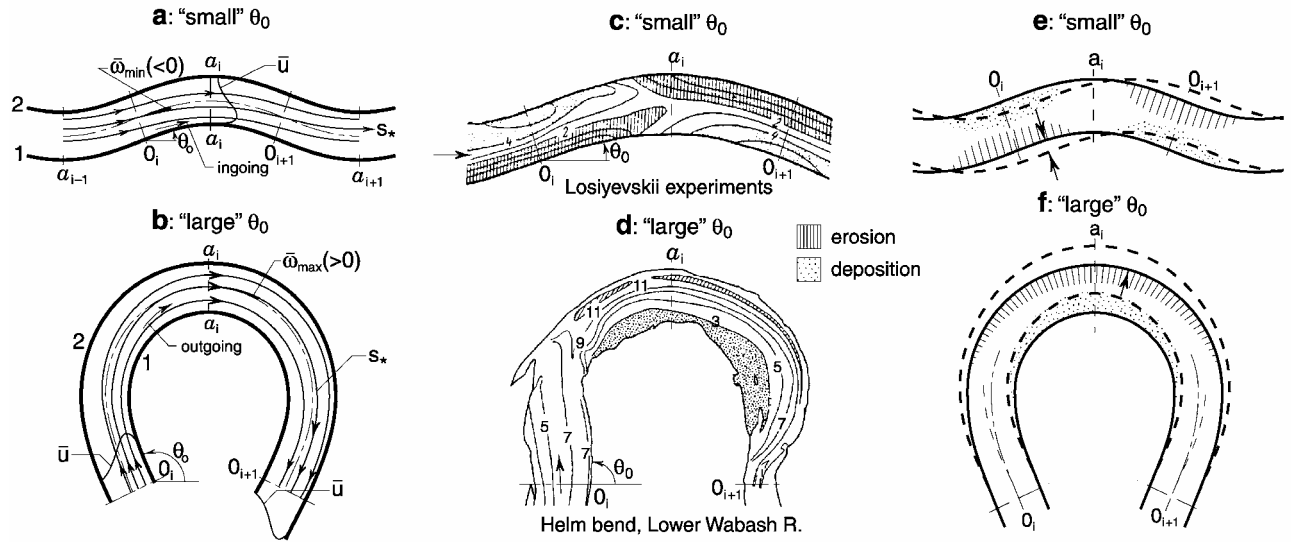


Figure 14 Flow convergence-divergence zones (a and b), bed erosion-deposition zones (c and d) and patterns of bank shifting (e and f) in streams having “small” and “large”  $\theta_0$ . (a), (b), (e) and (f) Schematical representations; (c) and (d) Measured by Losiyevskii (and reported by Kondratiev *et al.* 1982) and Jackson 1975, respectively

Hence the deepest erosions and highest depositions must be expected to occur around the crossovers  $O_i$  if  $\theta_0$  is “small”, and around the apex-sections  $a_i$  if  $\theta_0$  is “large”. The examples of actual streams shown in Figs. 14(c) and (d) appear to confirm that this is indeed so. Clearly, the banks must be eroded mostly in those locations where the bed adjacent to them is eroded; and similar reasoning applies to deposition. Therefore one must expect mainly migration for “small”  $\theta_0$ , and mainly expansion for “large”  $\theta_0$ , as illustrated in Figs. 14(e) and (f).

iv) The considerations in this section give rise to the following expectations:

1. All other conditions remaining the same, the location in plan of the [CD]’s should vary with  $\theta_0$  as shown in the schematic Fig. 15 (where the meandering channels are “straightened” for the sake of simplicity and “CONV” and “DIV” indicate the regions of flow convergence and divergence, respectively). Note that the shaded [CD] – having  $\bar{\omega} > 0$  – is centered around the crossover-section  $O_{i+1}$  for “small”  $\theta_0$ . Then its location gradually shifts upstream as  $\theta_0$  increases (as implied by the arrow), so that for “large”  $\theta_0$  it becomes centered around  $a_i$ ;
2. Consequently, the location of [ED]’s should vary with  $\theta_0$  as shown also in Fig. 15. The [ED], just like the [CD] which brought it into being, is centered around the crossover-section  $O_{i+1}$  for “small”  $\theta_0$ . Then its location gradually shifts upstream as  $\theta_0$  increases (as implied by the arrow), so that for “large”  $\theta_0$  it becomes centered around  $a_i$ .

[In Fig. 15,  $\xi_{c0}$  is the normalized (by  $L$ ) distance from the crossover  $O_i$  to the upstream end of the [CD] shown, while  $\lambda$  is the normalized (by  $L$ ) distance from the apex  $a_i$  to the mid-section of the erosion-deposition zone brought into being by the aforementioned [CD]. Both  $\xi_{c0}$  and  $\lambda$  are measured along the channel centreline].

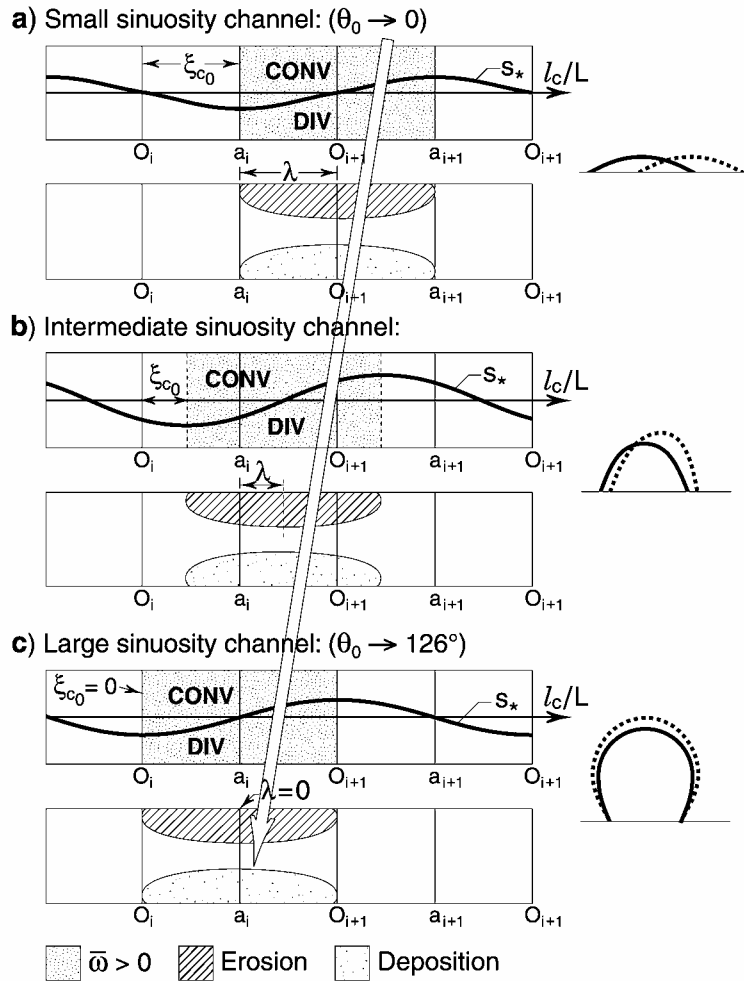


Figure 15 Variation with  $\theta_0$  of location of convergence-divergence flow zones and erosion-deposition zones

It should be clear that if the location in flow plan of [ED]’s is to vary with  $\theta_0$  as shown in Fig. 15, then this must necessarily lead to a combination of migration and expansion for “intermediate” values of  $\theta_0$ , with migration dominating when  $\theta_0$  is “small” and expansion dominating when  $\theta_0$  is “large” – which is in agreement with the migration/expansion patterns implied by Fig. 12.

A series of measurements carried out by da Silva *et al.* (In Press) in laboratory sine-generated channels having  $\theta_0 = 30^\circ, 50^\circ, 70^\circ, 90^\circ,$  and  $110^\circ$  ( $B = 0.40$  m;  $h \approx 3$  cm) and a flat sand bed ( $D_{50} = 2.2$  mm) seems to validate expectation 1. Indeed, consider the plot of the measured values of  $\xi_{c0}$  versus  $\theta_0$  in Fig. 16, and observe how the measured  $\xi_{c0}$  gradually decreases from 0.25 to 0 as  $\theta_0$  increases from  $0^\circ$  to  $138^\circ$ .

A recent analysis presented in da Silva and El-Tahawy (In Press) of all the available bed topography data from laboratory experiments in sine-generated channels, including that from a series of tests carried out by El-Tahawy (2004), appears to validate expectation 2.

The maximum value  $(\bar{\omega}_c)_{\max}$  of the deviation angles measured along the channel centreline of each of the aforementioned five channels is plotted versus  $\theta_0$  in Fig. 17. Note that the  $(\bar{\omega}_c)_{\max}$  - curve (the solid line passing through the measured values of  $(\bar{\omega}_c)_{\max}$ ) first increases as  $\theta_0$  increases, reaches its maximum, and then decreases. Clearly, as the deviation of  $\theta_0$  from  $\approx 70^\circ$  decreases,

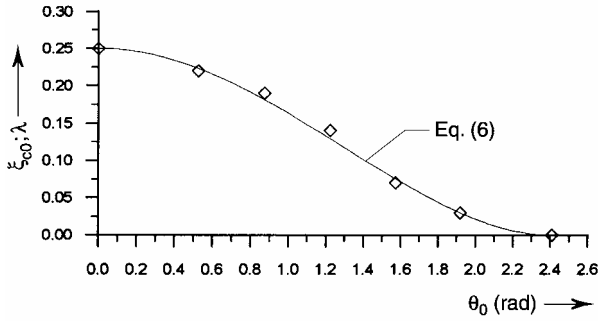


Figure 16 Plot of measured values of  $\xi_{c0}$  versus  $\theta_0$  (Eq. numbers are those in da Silva *et al.* (In Press))

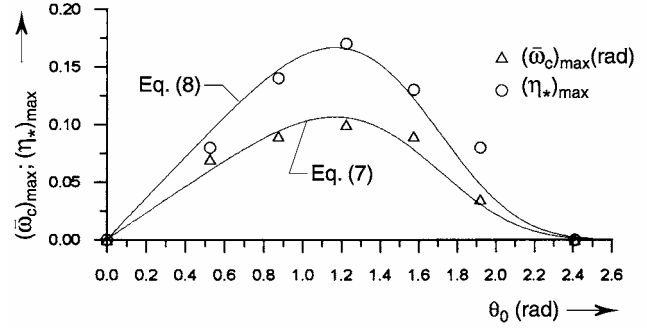


Figure 17 Plot of measured values of  $(\bar{\omega}_c)_{max}$  versus  $\theta_0$  (Eq. numbers are those in da Silva *et al.* (In Press))

$(B/R)_a$  increases (see Fig. 3(a)). But this means that the flow becomes “stronger” (in the sense that superelevation increases, velocity gradients increase, the amplitude of oscillation of  $s_*$  around the channel centreline increases, etc.). Therefore  $(\bar{\omega}_c)_{max}$  must necessarily increase – which explains why in Fig. 17  $(\bar{\omega}_c)_{max}$  reaches its maximum for  $\theta_0 \approx 70^\circ = 1.22$  rad.

I would like to end my lecture by pointing out that the maximum lateral expansion velocity occurs for values of  $\theta_0$  that are comparable with those for which  $(\bar{\omega}_c)_{max}$  is the largest (see Figs. 12 and 17). Clearly, the stronger the “intensity” of convergence-divergence of flow (i.e. the larger the value of  $(\bar{\omega}_c)_{max}$ ), the deeper will be the erosions at the bed and the stronger the direct action of flow on the banks – and, consequently, the larger the lateral expansion velocity.

Thank you very much for your attention.

## Acknowledgements

I would like to express my thanks to Dr. M.S. Yalin, Emeritus Professor, Queen’s University, with whom I have been working since 1989, and who was always a tremendous source of inspiration and motivation. I would also like to thank Dr. T.J. Harris, Dean of the Faculty of Applied Science, Queen’s University, who greatly contributed to the establishment of my current research program at Queen’s. Finally, but not least, I thank all my former and present graduate students, for their many contributions and boundless enthusiasm.

## Notation

- $A_*$  = energy-related property of flow (subjected to minimization during the regime channel formation)
- $B$  = flow width
- $c$  = dimensionless (Chézy) resistance factor
- $D$  = typical grain size (usually  $D_{50}$ )
- $Fr$  = flow Froude number
- $h$  = flow depth
- $J_0(\theta_0)$  = Bessel function of first kind and zero-th order (of  $\theta_0$ )
- $k_s$  = granular roughness of bed surface ( $k_s \approx 2D_{50}$ )
- $l$  = longitudinal coordinate;  $l = 0$  at the crossover  $O_i$  (see Fig. 1)

- $L$  = meander length (measured along  $l_c$ )  
 $l_c$  = longitudinal coordinate along the centreline of a meandering flow;  $l_c = 0$  at the crossover  $O_i$  (see Fig. 1)  
 $p$  = porosity of granular material  
 $Q$  = flow rate  
 $\mathbf{q}_s$  = specific volumetric bed-load rate vector  
 $R$  = curvature radius of the centreline of a meandering flow  
 $Re$  = flow Reynolds number ( $= hu_{av}/\nu$ )  
 $S$  = bed slope  
 $s_*$  = streamline that divides the flow rate  $Q$  in two equal (left and right) parts (see Fig. 13)  
 $t$  = time  
 $T_V, T_H$  = development duration of vertical and horizontal bursts, respectively  
 $T_R$  = development duration of the regime channel  
 $u_{av}$  = channel-averaged flow velocity  
 $\bar{u}$  = vertically-averaged longitudinal flow velocity  
 $\bar{U}$  = magnitude of the vertically-averaged local flow velocity vector  $\mathbf{U}$   
 $v_*$  = shear velocity ( $= \sqrt{\tau_0 / \rho}$ )  
 $\bar{v}_r$  = average radial velocity of the cross-circulatory flow directed towards inner bank  
 $W$  = local displacement velocity of the meandering bed surface (in the vertical direction)  
 $x$  = direction of rectilinear flow; also general direction of meandering flow  
 $y$  = direction horizontally perpendicular to  $x$   
 $z$  = Vertical direction  
 $z_b$  = bed elevation measured with regard to an arbitrary reference datum  
 $\gamma$  = fluid specific weight  
 $\theta, \theta_0$  = deflection angle of a meandering flow at any  $l_c$  and at  $l_c = 0$ , respectively (see Fig. 1)  
 $\lambda$  = dimensionless longitudinal coordinate, measured along  $l_c$  from the apex-section  $a_i$ , of the cross-section where (within a loop  $O_i a_i O_{i+1}$ ) maximum erosion-deposition occurs (see Fig. 15)  
 $\lambda_V, \lambda_H$  = length of vertical and horizontal bursts, respectively  
 $\Lambda_i$  = length of bed form  $i$  ( $i = d$  if dunes;  $i = a$  if alternate bars)  
 $\Lambda_M$  = meander wavelength  
 $\nu$  = fluid kinematic viscosity  
 $\xi_c$  = dimensionless counterpart of  $l_c$  ( $\xi_c = l_c / L$ )  
 $\xi_{c0}$  = dimensionless longitudinal coordinate, measured along  $l_c$  from the crossover  $O_i$ , of the upstream-end of a  $L/2$ -long convergence-divergence flow zone where  $\bar{\omega} > 0$  (see Fig. 15)  
 $\rho$  = fluid density  
 $\sigma$  = sinuosity of a meandering flow ( $\sigma = L / \Lambda_M$ )  
 $\tau_0$  = bed shear stress  
 $\bar{\omega}$  = deviation angle (angle between the vertically-averaged streamline  $s$  and the coordinate line  $l$  of a meandering flow)  
 $\bar{\omega}_c$  = value of  $\bar{\omega}$  at the centreline of a meandering flow

**Subscripts:**

- $0$  marks the value of a quantity at time  $t = 0$   
 $a$  marks the value of a quantity at the apex-section of a meandering stream  
 $av$  marks the channel-averaged value of a quantity  
 $max$  marks the maximum value of a quantity  
 $R$  marks the regime value of a quantity

## References

1. ACKERS, P. (1964). "Experiments on small streams in alluvium". *J. Hydr. Div. ASCE*, Vol. 90, No. HY4.
2. BETTESS, R. and WHITE, W.R. (1983). "Meandering and braiding of alluvial channels". *Proc. Instn. Civ. Engrs.*, Part 2, 75, Sept.
3. BLACKWELDER, R.F. (1978). "The bursting process in turbulent boundary layers". *Lehigh Workshop on Coherent Structures in Turbulent Boundary Layers*.
4. CANTWELL, B.J. (1981). "Organised motion in turbulent flow". *Ann. Rev. Fluid Mech*, Vol. 13.
5. CHANG, H.H. (1988). "*Fluvial processes in river engineering*". John Wiley and Sons Inc., New York.
6. DA SILVA, A.M.F., EL-TAHAWY, T. and TAPE, W.D. "Variation of flow pattern with sinuosity in sine-generated meandering streams". *J. Hydraul. Engrg. ASCE* (In Press).
7. DA SILVA, A.M.F. and EL-TAHAWY. "Location of hills and deeps in meandering streams: an experimental study". *Proc. River Flow 2006, Int. Conf. on Fluvial Hydraulics*, Lisbon, September 2006 (In Press).
8. DA SILVA, A.M.F. (1995). "*Turbulent flow in sine-generated meandering channels*". Ph.D. Thesis, Dept. of Civil Engrg., Queen's Univ., Kingston, Canada.
9. DA SILVA, A.M.F. (1991). "*Alternate bars and related alluvial processes*". M.Sc. Thesis, Queens' University, Kingston, Canada.
10. DE LELIAVSKY, N. (1894). "Currents in streams and the formation of stream beds". *Sixth International Congress on Internal Navigation*, The Hague, The Netherlands.
11. DEMENTIEV, M.A. (1962). "*Investigation of flow velocity fluctuations and their influences on the flow rate of mountainous rivers*". (In Russian) Tech. Report of the State Hydro-Geological Inst. (GGI), Vol. 98.
12. EL-TAHAWY, T. (2004). "*Patterns of flow and bed deformation in meandering streams: an experimental study*". Ph.D. Thesis, Queens' University, Kingston, Canada.
13. ENGELS, H. (1926). "Movement of sedimentary materials in river bends". In *Hydraulic Laboratory Practice*, J.R. Freeman ed., New York, ASME.
14. FARGUE, L. (1908). "La forme du lit des rivières à fond mobile". Gauthier-Villars, Paris.
15. FRIEDKIN, J.F. (1945). "A laboratory study of the meandering of alluvial rivers" U.S. Waterways Exp. Sta., Vicksburg, Mississippi.
16. GAD-EL-HAK, M. and HUSSAIN, A.K.M.F. (1986). "Coherent structures in a turbulent boundary layer". *Phys. Fluids*, Vol. 29, July.
17. GARDE, R.J. and RAJU, K.G.R. (1977). "*Mechanics of sediment transportation and alluvial stream problems*". Wiley Eastern, New Dehli.
18. GRISHANIN, K.V. (1979). "*Dynamics of alluvial streams*". (In Russian) Gidrometeoizdat, Leningrad.
19. HAYASHI, T. (1971). "Study of the cause of meanders". *Trans. JSCE*, Vol. 2, Part 2.
20. HOOKE, R.L. (1974). "*Distribution of sediment transport and shear stress in a meander bend*". Rept. 30, Uppsala Univ. Naturgeografiska Inst., 58.
21. HUSSAIN, A.K.M.F. (1983). "Coherent structures – reality and myth". *Phys. Fluids*, Vol. 26, Oct.
22. INGLIS, C.C. 1947. "Meanders and their bearing on river training". *Maritime and Waterways Engrg. Div., Inst. Civ. Eng.*, London.
23. JACKSON, R.J. (1975). "Velocity-bed-form-texture patterns of meander bends in the lower Wabash River of Illinois and Indiana." *Geol. Soc. Am. Bull.*, Vol. 86, Nov.
24. JEFFERSON, M. (1902). "The limiting width of meander belts". *National Geographic Magazine*, Oct., 372-384.
25. JIA, Y. (1990). "Minimum Froude number and the equilibrium of alluvial sand rivers". *Earth Surf. Processes and Landforms*, Vol. 15.
26. JSCE Task Committee on the Bed Configuration and Hydraulic Resistance of Alluvial Streams (1973). "The bed configuration and roughness of alluvial streams". (In Japanese) *Proc. JSCE*, No. 210, Feb.
27. KALKWIJK, J.P.TH. and DE VRIEND, H.J. (1980). "Computation of the flow in shallow river bends." *J. Hydraul. Res.*, 18(4), 327-342.
28. KARCZ, I. (1971). "Development of a meandering thalweg in a straight erodible laboratory channel". *J. Geology*, Vol. 79.

29. KLAIVEN, A.B. 1966. "Investigation of structure of turbulent streams". Tech. Report of the State Hydro-Geological Inst. (GGI), Vol. 136.
30. KONDRATIEV, N., POPOV, I., SNISHCHENKO, B. (1982). "Foundations of hydromorphological theory of fluvial processes". (In Russian) Gidrometeoizdat, Leningrad.
31. LANGBEIN, W.B. and LEOPOLD, L.B. (1966). "River meanders – theory of minimum variance". *U.S. Geol. Survey Prof. Paper* 422-H, 1-15.
32. LELIAVSKY, S. (1959). "An introduction to fluvial hydraulics". Constable and Company.
33. LEOPOLD, L.B. and LANGBEIN, W.B. (1966). "River meanders". *Sci. Am.*, 214(6), 60-70.
34. LEOPOLD, L.B., WOLMAN, M.G. and MILLER, J.P. (1964). "Fluvial processes in geomorphology". W.H. Freeman, San Francisco.
35. LEOPOLD, L.B. and WOLMAN, M.G. (1957). "River channel patterns: braided, meandering and straight". *U.S. Geol. Survey Professional Paper* 282-B.
36. MAKAVEYVEV, N.I. (1975). "River bed and erosion in its basin". Press of the Academy of Sciences of the USSR, Moscow.
37. MATTHES, G.H. (1941). "Basic aspects of stream meanders." *Trans. Am. Geophys. Union*, 632-636.
38. NELSON, J. M. and SMITH, J. D. (1989). "Evolution and stability of erodible channel beds." In *River Meandering*, S. Ikeda and G. Parker eds., Am. Geophys. Union, Water Resour. Monograph, 12, 321-378.
39. NEZU, I. and NAKAGAWA, H. (1993). "Turbulence in open-channel flows". IAHR Monograph, A.A. Balkema, Rotterdam, The Netherlands.
40. RASHIDI, M. and BANERJEE, S. (1988). "Turbulence structure in free-surface channel flows". *Phys. Fluids, Vol. 31, Sept.*
41. SHIMIZU, Y. (1991). "A study on prediction of flows and bed deformation in alluvial streams". (In Japanese) Civ. Eng. Res. Inst., Hokkaido Development Bureau, Sapporo, Japan.
42. SMITH, J.D. and MCLEAN, S.R. (1984). "A model for flow in meandering streams". *Water Resour. Res.*, 20(9), 1301-1315.
43. STRUIKSMA, N. and CROSATO, A. (1989). "Analysis of a 2-D bed topography model for rivers." *River Meandering*, S. Ikeda and G. Parker eds., Am. Geophys. Union, Water Resour. Monograph, 12, 153-180.
44. TERMINI, D. (1996). "Evolution of a meandering channel with an initial flat bed. Theoretical and experimental study of the channel bed and the initial kinematic characteristics of flow". (In Italian) Ph.D. Thesis, Dept. Hydraulic Engineering and Environmental Applications, University of Palermo, Italy.
45. THOMSON, J. (1879). "On the flow of water round river bends". *Proc. Inst. Mech. Eng.*, Aug. 6.
46. VELIKANOV, M.A. (1958). "Alluvial processes (fundamental principles)". (In Russian) State Publishing House for Physical and Mathematical Literature, Moscow.
47. VELIKANOV, M.A. (1955). "Dynamics of alluvial streams". (In Russian) Gostechizdat, Moscow.
48. WHITING, P.J. and DIETRICH, W.E. (1993). "Experimental studies of bed topography and flow patterns in large-amplitude meanders. 2. Mechanisms". *Water Resour. Res.*, 29(11), 3615-3622.
49. YALIN, M.S. and DA SILVA, A.M.F. (2001). "Fluvial Processes". IAHR Monograph, IAHR, Delft, The Netherlands.
50. YALIN, M.S. (1992). "River Mechanics". Pergamon Press, Oxford.
51. YALIN, M.S. (1977). "Mechanics of sediment transport". Pergamon Press, Oxford.
52. YANG, C.T., SONG, C.C.S. and WOLDENBERG, M.J. (1981). "Hydraulic geometry and minimum rate of energy dissipation". *Water Resour. Res.*, 17.
53. YANG, C.T. (1971). "On river meanders". *J. Hydrology*, 13.
54. YOKOSI, S. (1967). "The structure of river turbulence". Bull. Disaster Prevention Res. Inst., Kyoto Univ., Vol. 17, Part 2, No. 121, Oct.
55. ZELLER, J. (1967). "Meandering channels in Switzerland". *Int. Symp. on River Morphology*, Bern, IASH.